Magnetic and Magneto-Optical Properties of NiMnSb1-xSnx Compounds in Relation to their Electronic Band Structure

Groot, R.A. de; Engen, P.G. van; Engelen, P.P.J. van; Buschow, K.H.J.

Published in:
Journal of Magnetism and Magnetic Materials

DOI:
10.1016/0304-8853(90)90140-L

Publication date:
1990

Journal of Magnetism and Magnetic Materials 86 (1990) 326–332
North-Holland

MAGNETIC AND MAGNETO-OPTICAL PROPERTIES OF $NiMnSb_{1-x}Sn_x$ COMPOUNDS IN RELATION TO THEIR ELECTRONIC BAND STRUCTURE

R.A. de GROOT

Faculty of Sciences, Toernooiveld, 6525 ED Nijmegen, The Netherlands

P.G. van ENGEN, P.P.J. van ENGELEN and K.H.J. BUSCHOW

Philips Research Laboratories, 5600 JA Eindhoven, The Netherlands

Received 11 September 1989

We have determined the magnetic and magneto-optical properties of pseudoternaries of the type $NiMnSb_{1-x}Sn_x$. These materials were found to have the cubic MgAgAs structure ($C1_b$) for concentrations where $x \leq 0.7$. Lattice constants, saturation moments, Curie temperatures and magneto-optical Kerr rotations (0.5–4.5 eV) were found to vary smoothly with x, which makes it possible to derive by extrapolation values of all these physical constants for the fictitious compound NiMnSn. Calculations of the electronic band structure were made for NiMnSn and $NiMnSb_{0.75}Sn_{0.25}$. These calculations and those presented earlier for NiMnSb were used to analyse the magnetic and magneto-optical properties of the compounds $NiMnSb_{1-x}Sn_x$.

1. Introduction

In a previous investigation the very high magneto-optical Kerr effect of PtMnSb was studied. It was shown that the high Kerr rotation of this compound is related to its unusual electronic properties [1]. PtMnSb belongs to the class of compounds having the cubic MgAgAs structure ($C1_b$ structure) which is adopted also by NiMnSb. The electronic band structure of both compounds can be characterized as exhibiting metallic behaviour in one spin direction and semiconducting behaviour in the other [2]. In the present study we report on the magnetic and magneto-optical properties of compounds of the series $NiMnSb_{1-x}Sn_x$. The interest in these materials has resulted from features of the electronic band structure of NiMnSb. Results of band structure calculations [2] are given in fig. 1, showing the energy gap around the Fermi energy E_F in the band structure of the minority spin electrons. A detailed analysis of the magneto-optical properties associated with materials having this type of electronic structure revealed that a large Kerr rotation can be expected when the valence-band Γ_4 states in fig. 1b come very close to E_F, as found in PtMnSb [1]. The present investigation was prompted mainly by practical considerations. By continuously lowering E_F in NiMnSb via substitution of Sn for Sb, up to a point where the Γ_4 states would touch E_F, it was hoped one could synthesize a material possessing magneto-optical properties at least as favourable as those of PtMnSb. Another important reason for studying $NiMnSb_{1-x}Sn_x$ was to test the model for the magneto-optical properties proposed earlier, while at the same time placing this model on a broader experimental basis.

2. Experimental

Various samples of the series $NiMnSb_{1-x}Sn_x$ were prepared by arc melting, followed by vacuum annealing at 800 °C for 2 weeks. X-ray diffraction

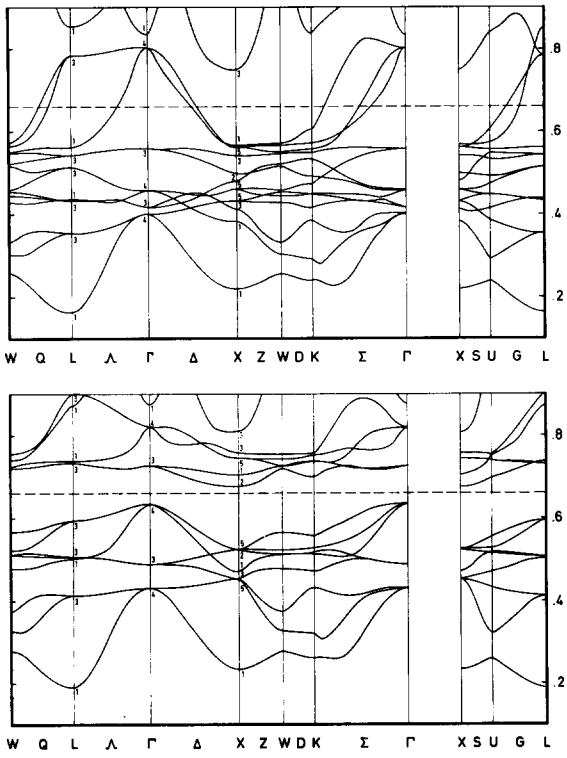

Fig. 1. Electronic band structure of NiMnSb. (a) majority-spin direction; (b) minority-spin direction. The energy on the vertical axes is in rydberg units.

showed that the samples were almost single phase, the amount of second phases being of the order of 5%.

Magnetic measurements were made in the range 4.2–900 K with magnetic field strengths up to 1440 kA m^{-1} by means of the Faraday method. The Curie temperatures (T_c) were determined from the temperature dependence of the magnetization (σ) measured in low fields ($H \leq 80$ kA m^{-1}) by plotting σ^2 versus T and extrapolating the linear part to $\sigma^2 = 0$.

The polar Kerr rotation (φ_K) and ellipticity (ϵ_K) were measured at room temperature in the range 0.5–4.5 eV. Low-frequency polarization modulation, by means of a Faraday modulator, enabled phase-sensitive detection to be used. For the determination of the Kerr ellipticity we used several quarterwave plates, the retardation of which had been carefully measured as a function of photon energy. All magneto-optical measurements were made on flat portions of the samples, polished with diamond paste. The magnetization direction was kept perpendicular to the optical surface by means of a magnetic field of 920 kA m^{-1}. In practice, the mean angle of incidence of the light beam on the sample surface had to be 4.5°.

3. Experimental results

Results of the X-ray diffraction measurements made on $NiMnSb_{1-x}Sn_x$ showed that the cubic Cl_b structure exists up to $x = 0.7$. The lattice constant (a) is plotted as a function of concentration in fig. 2. It is seen that the values of a increase linearly with x and extrapolate to the value $a = 0.6025$ for NiMnSn.

From the magnetic isotherms measured at 4.2 K, values of the saturation magnetization were derived. These values, expressed in Bohr magne-

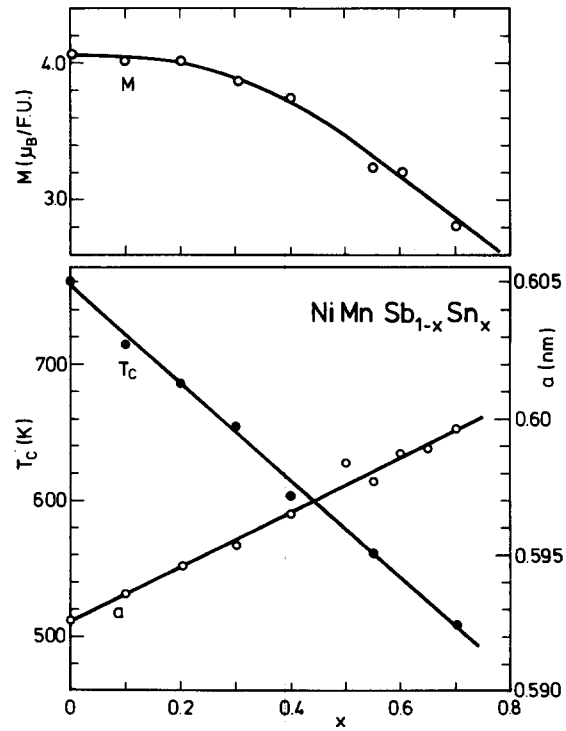

Fig. 2. Concentration dependence of the saturation moment (M) at 4.2 K, the Curie temperature (T_C) and the lattice constant (a) in Cl_b-type $NiMnSb_{1-x}Sn_x$ compounds.

tons per formula unit, are plotted as a function of concentration in the top part of fig. 2. Up to $x = 0.2$ the increase in Sn concentration does not lead to significant changes of moment. For Sn concentrations higher than $x = 0.4$ the saturation moment decreases strongly. Linear extrapolation to $x = 1$ leads to a value of $(2.0 \pm 0.3)\mu_B$ appropriate to the hypothetical NiMnSn. The concentration dependence of the Curie temperatures in $NiMnSb_{1-x}Sn_x$ is shown in the lower part of fig. 2. The values of T_c are seen to decrease linearly with x. By extrapolation, the Curie temperature for NiMnSn is found to be 406 K.

Results of magneto-optical measurements made at room temperature are given for three representative concentrations in fig. 3 In NiMnSb the Kerr spectrum exhibits two strong $|\varphi_K|$ peaks, one near 1.4 eV and the other near 3.8 eV. In the intermediate energy range the values of $|\varphi_K|$ remain rather low. The same features are apparent

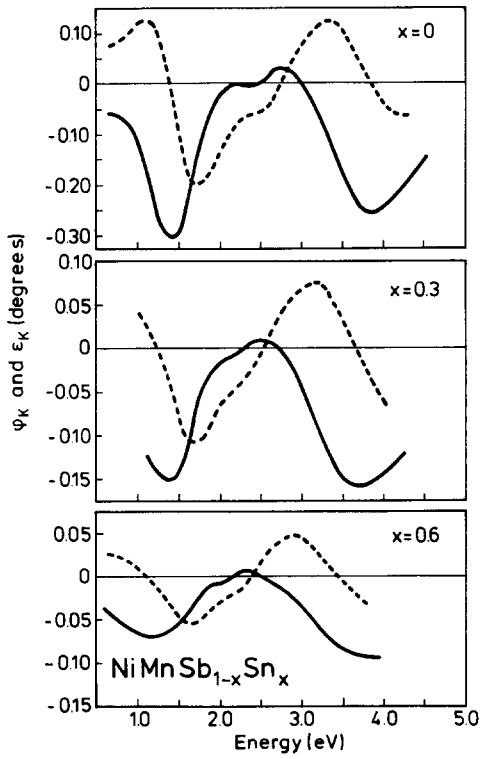

Fig. 3. Kerr rotation angle (φ_K, full curves) and ellipticity (ϵ_K, dashed curves) as a function of photon energy for three compounds of the series $NiMnSb_{1-x}Sn_x$.

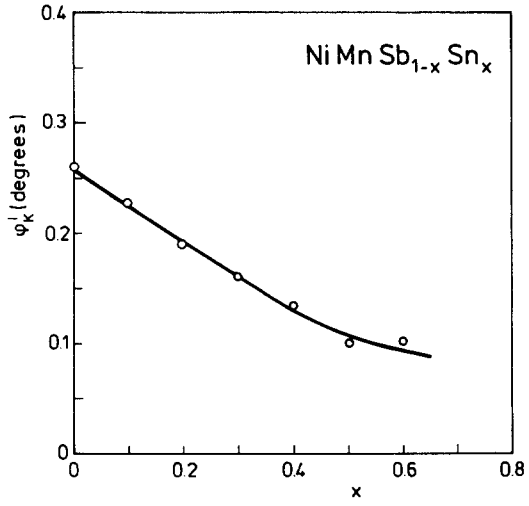

Fig. 4. Concentration dependence of the reduced polar Kerr rotation angle $\varphi'_K = \varphi_K\,[\sigma(4.2\text{ K})/\sigma(300\text{ K})]$.

in the spectra of the pseudobinary compounds, the only differences being a broadening of the peaks and a tendency of these peaks to shift to lower photon energies. Moreover, the intensities of the peaks become strongly reduced with increasing Sn concentration. Part of the decrease in intensity is due to the decrease of the room temperature magnetization with Sn concentration in the $NiMnSb_{1-x}Sn_x$ compounds. In order to correct for the latter effect we have plotted in fig. 4 the concentration dependence of the reduced value of the low-energy peak intensity defined as $\varphi'_K = \varphi_K\,[\sigma(4.2\text{ K})/\sigma(300\text{ K})]$. After this correction the peak intensities are still seen to decrease markedly with Sn concentration. In the remainder of this paper we will restrict ourselves to discussing the low-energy peak.

4. Band structures

Calculations of the electronic band structure of NiMnSb have been given in a previous publication [2]. In order to discuss the magnetic and magneto-optical properties of the series of $NiMnSb_{1-x}Sn_x$ compounds, similar calculations for NiMnSn were made, although it has been found that this compound is not stable in its pure form. For the band-structure calculations, we used

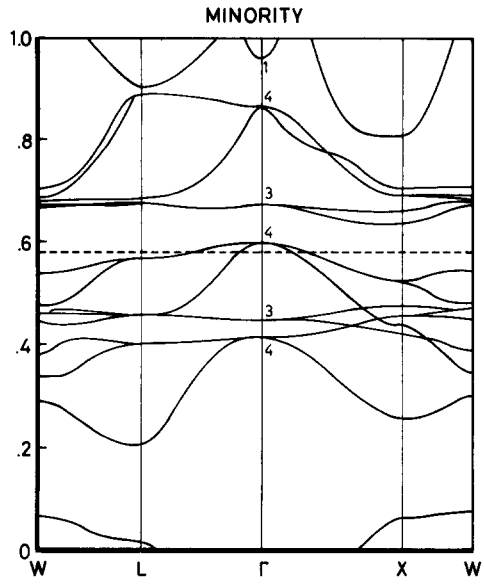

Fig. 5. Electronic band structure for minority-spin electrons in NiMnSn. The energy scale on the vertical axis is in rydberg units.

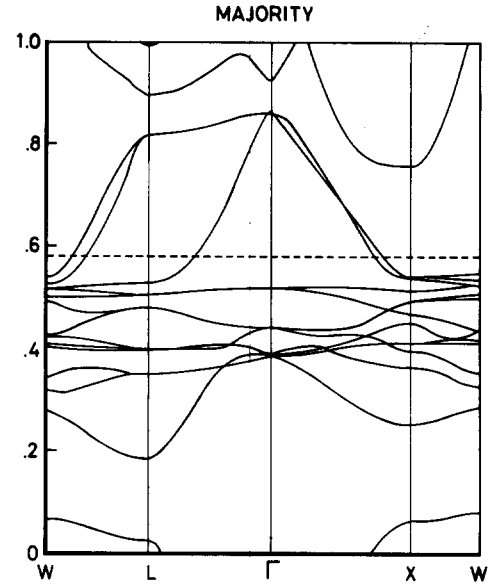

Fig. 6. Electronic band structure for majority-spin electrons in NiMnSn. The energy scale on the vertical axis is in rydberg units.

the extrapolated lattice constant $a = 0.6025$ nm derived for NiMnSn in the previous section. The calculations were performed by means of the self-consistent augmented-spherical-wave (ASW) method of Williams, Kübler and Gelatt [3], including scalar relativistic effects as described by Methfessel and Kübler [4]. The unoccupied $\frac{1}{2}, \frac{1}{2}, \frac{1}{2}$ positions in the Cl_b-type crystal structure of NiMnSn were treated as atoms with zero nuclear charge [5].

From the results of the calculations it was inferred that the use of the quasi-empirically determined lattice constant for NiMnSn leads to an acceptable pressure. For this reason no attempts were made to minimize the total energy as a function of the lattice constant.

The band structure for the majority and minority spin directions is shown in figs. 5 and 6, respectively. The energy dependence of the density of states is given in fig. 7. There is a close resemblance with the band structure of NiMnSb (fig. 1).

Band-structure calculations were made also for the concentration $x = 0.25$ of the series $NiMnSb_{1-x}Sn_x$. This compound was regarded as having a hypothetical structure in which the substitution

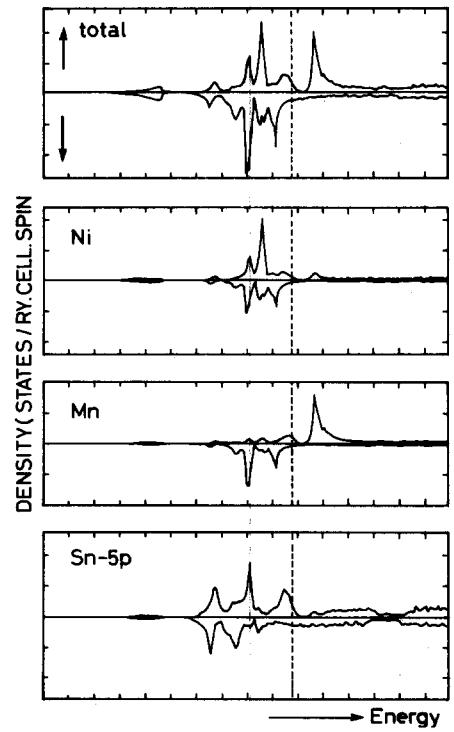

Fig. 7. Density of states derived from band-structure calculations for NiMnSn.

of Sn atoms has not occurred at random. Per unit cell NiMnSb, only a single Sn is substituted into one of the four possible crystallographic Sb sites, this site being the group Pm3 or T^1 with Sn in the Wyckoff positions 1a, Sb in 3c, Mn in 1b and 3d, and Ni in 4e (with atomic position parameter $x = \frac{3}{4}$). In fact, this structure allows the highest concentration of substituted Sn atoms without the occurrence of Sn atom pairs. From the results of the band-structure calculations we derive that the valence band has closely approached E_F at Γ. There are no split-off Sn states, from which it may be assumed that there is no risk of finding split-off states from the valence band in the system $NiMnSb_{1-x}Sn_x$.

5. Discussion

Inspection of the band structures for the majority and minority spin directions in NiMnSn (figs. 5 and 6) shows that this material is a ferromagnetic metal, since electron bands intersect the Fermi level in both spin directions. The spectacular feature present in NiMnSb, where the minority band structure has an energy gap straddling the Fermi surface (fig. 1b), is absent in NiMnSn. On the other hand, comparison of the band structure of NiMnSb with that of NiMnSn shows that there is a close resemblance, the main difference being that the relative position of the Fermi level has decreased in the latter material. This is plausible since Sn has one p electron less than Sb.

Furthermore, the differences between the electronic band structure of the two compounds entails lower magnetic moments at the Ni and Mn sites in NiMnSn than in NiMnSb. The absolute value of the Sn moment in NiMnSn is larger than the corresponding value of the Sb moment in NiMnSb. Numerical data obtained from the band-structure calculations are given in table 1. By extrapolation one would find an experimental value for the total moment which is lower than that derived from the band-structure calculations.

We will now discuss the magneto-optical properties of $NiMnSb_{1-x}Sn_x$, using the model proposed earlier to explain the huge Kerr rotation in the $C1_b$ type compound PtMnSb [1]. The band

Table 1
Magnetic moments (in μ_B per atom) calculated for the various atoms in NiMnSb and NiMnSn. The total calculated moment M_{calc} and the corresponding experimental value M_{exp} are given in μ_B er formula unit. The experimental value for the non-existent NiMnSn was derived by extrapolation (see text)

NiMnX	M_{Ni}	M_{Mn}	M_X	M_{calc}	M_{exp}
X = Sb	0.31	3.73	−0.04	4.00	4.03
X = Sn	0.10	3.48	−0.21	3.37	2.0±0.3

structure of the latter compounds is in many respects similar to that described above for NiMnSb and NiMnSn. Like NiMnSb, the compound PtMnSb can be characterized as a half-metallic ferromagnet, the top of the minority-spin valence band Γ_4 being primarily composed of Sb p states. However, since the top of the valence band is rather close to E_F in PtMnSb, the effect of spin–orbit interaction, which splits the degenerate Γ_4 state into three singlet states ($m = 0$, $m = \pm 1$), pushes the $m = +1$ state to above the Fermi level. This latter state, now being empty, can no longer serve as initial state for the magneto-optical transitions from Γ_4 to Γ_1 and from Γ_4 to Γ_2, where Γ_1 and Γ_3 are both situated above E_F (see fig. 8). In

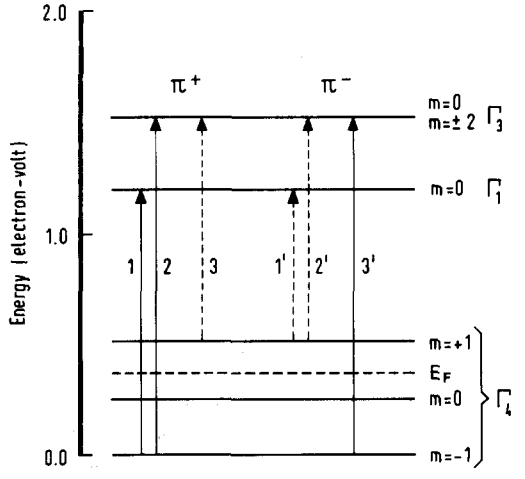

Fig. 8. Energy levels in the vicinity of the Fermi energy for the minority-spin direction in PtMnSb. The arrows represent the various allowed optical transitions. The dashed lines pertain to transitions that are possible only when the $m = +1$ state is populated with electrons, i.e., when E_F is lying at a higher energy than the $m = +1$ state.

fact, it means that the intensity of the transitions starting from the $m = -1$ state of Γ_4 (full arrows in fig. 8) will no longer be compensated by the contribution of states starting from the $m = +1$ state (broken arrows in fig. 8). The beneficial influence of this particular location of E_F in between $m = -1$ and $m = +1$ of Γ_4 on the total Kerr intensity is obvious. The transition indicated by 1 in fig. 8 has by far the largest oscillator strength [1].

In this model, the exact position of the Fermi energy with respect to the top of the valence band is of importance [6]. It is exactly this quantity which one can hope to adjust in a rigid-band-like manner by the partial substitution of Sn for Sb in NiMnSb. The occurrence of the band gap, its size and the position with respect to E_F have been studied by Van der Heide et al. [7]. They conclude that the situation with the band gap is in agreement with the calculations for PtMnSb. But they find a smaller bandgap for NiMnSb. This can be interpreted as meaning that the situation in NiMnSb near E_F is not far off from that in PtMnSb, in contrast with the calculations. This already suggests that no benefit is to be expected from the substitution of Sn for Sb in NiMnSb. Our magneto-optical spectra seem to confirm this conclusion.

In optical excitations, final states are as important as initial states. The very high Kerr rotation in PtMnSb is not just a consequence of the favourable position of the Fermi energy with respect to the spin–orbit split valence band. Also, the final states are very favourable in PtMnSb. The final state of symmetry Γ_1 in PtMnSb has exactly the correct excitation energy and also exhibits an extremely favourable combination of oscillator strength and joint density of states. It is precisely here that the largest differences between NiMnSb and PtMnSb occur. The final state Γ_1 in NiMnSb is positioned at a much higher energy and also the optical excitation between the top of the valence band and the Γ_1 level is much less intense.

This leaves the intensity contributions of the off-diagonal part of the dielectric tensor at the excitation energy of 1–2 eV to the transitions between Γ_4 and Γ_3. These are, however, an order of magnitude less intense than those of the transitions terminating at Γ_1.

By inspecting the band-structure calculation for NiMnSn, it can be concluded that there is a strong similarity in final states between NiMnSb and NiMnSn. The Γ_1 level, as in NiMnSb, is positioned at a much higher excitation energy than in PtMnSb and also shows a very strong dispersion. Thus, the optical transition from the top of the valence band Γ_4 to the final state level Γ_1 will again be weak.

Band-structure calculations performed by us on the system $NiMnSb_{0.75}Sn_{0.25}$ suggests that the substitution of Sb by Sn can be described in a smooth rigid-band-like manner. Nothing new can therefore be expected in $NiMnSb_{1-x}Sn_x$ with respect to the relative positions of the initial state Γ_4 and the final states Γ_3 and Γ_1. The only essential change taking place by the Sn substitution occurs with respect to the relative position of E_F. The reduction in electron concentration with Sn concentration will lead to a lowering of E_F. If we again assume that the relative position of E_F within the manifold of Γ_4 states in NiMnSb is roughly the same as it is in PtMnSb (fig. 8), one expects that the lowering of E_F will ultimately lead to a depopulation of the Γ_4 initial state. Consequently, the intensity of the Γ_4–Γ_3 transition is expected to decrease with x. The onset of this decrease in intensity would occur at the Sn concentration for which E_F falls just below the $m = -1$ level of Γ_4 if only vertical excitation plays a role. Furthermore, considerable smearing out will occur in view of the local nature of the excitation and the statistical distribution of Sn atoms over the Sb sites. Both effects will make the intensity reduction be a gradual one, as is observed experimentally (fig. 4).

There is still another mechanism which may come into play in the series $NiMnSb_{1-x}Sn_x$. In the discussion given above we have considered changes affecting the off-diagonal part (ϵ_{xy}) of the dielectric tensor only. This off-diagonal part enters the expression of the magneto-optical transitions in the numerator [8]. The diagonal part ϵ_{xx} of the dielectric tensor leads to a factor $\sqrt{\epsilon_{xx}}(1 - \epsilon_{xx})$ in the denominator. The disorder introduced by the Sn substitution has the effect of increasing the diagonal part of the dielectric tensor. As a

result, the term $\sqrt{\epsilon_{xx}}(1-\epsilon_{xx})$ may increase so that the Kerr rotation decreases with Sn concentration. Inspection of the data of fig. 3 shows that the intensity reduction with increasing Sn concentration affects the transition at about 1.5 and 4 eV in an roughly equal manner. However, it is unlikely that the Kerr intensity enhancement via the term $(1-\epsilon_{xx})^{-1}$ carries the same weight for both transitions. For this reason we believe that the effects of the diagonal term in explaining the reduction of φ_K with Sn concentration play only a minor role in the $NiMnSb_{1-x}Sn_x$ system considered here.

References

[1] R.A. de Groot, F.M. Mueller, P.G. van Engen and K.H.J. Buschow, J. Appl. Phys. 55 (1984) 2151.

[2] R.A. de Groot, F.M. Mueller, P.G. van Engen and K.H.J. Buschow, Phys. Rev. Lett. 50 (1983) 2024.

[3] A.R. Williams, J. Kübler and C.D. Gelatt Jr., Phys. Rev. B 19 (1979) 6094.

[4] M. Methfessel and J. Kübler, J. Phys. F 12 (1982) 141.

[5] R.B. Helmholdt, R.A. de Groot, F.M. Mueller, P.G. van Engen and K.H.J. Buschow, J. Magn. Magn. Mat. 43 (1984) 249.

[6] R.A. de Groot and K.H.J. Buschow, J. Magn. Magn. Mat. 54–57 (1986) 1377.

[7] P.A.M. van der Heide, W. Baelde, R.A. de Groot, A.R. de Vroomen, P.G. van Engen and K.H.J. Buschow, J. Phys. F 15 (1985) L75.

[8] H. Feil and C. Haas, Phys. Rev. Lett. 65 (1987) 58.